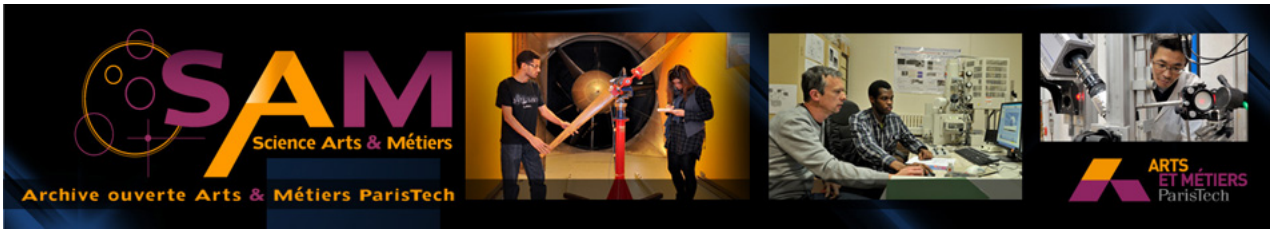

# Experimental Parameters Identification of Fatigue Damage Model for Short Glass Fiber Reinforced Thermoplastics GFRP

Hedi Nouri[1], Christophe Czarnota[2], and Fodil Meraghni[3]

[1] COHMAS-PSE,
King Abdullah University of Science and Technology,
Thuwal, Kingdom of Saudi Arabia
Hedi.nouri@kaust.edu.sa
[2] LEMTA, GIP-InSIC, 27 rue d'Hellieule,
88100 Saint-Dié-des-Vosges, France
[3] LEM3, Arts et Métiers ParisTech. - Metz,
4 Rue Augustin Fresnel, 57078 Metz, France

**Abstract.** In the present work, a new polycyclic fatigue damage model is formulated and applied for short glass fibre reinforced thermoplastics. The model is able to capture experimental trends observed for the considered composites. The damage growth description involves a set of 20 parameters in the case of a complete 3D –structure. In the current paper, it is considered the particular case of a displacement controlled fatigue tensile test involving 4 damage parameters. The present contribution is a first approach of parameter identification. It is considered a least squares sense based cost function and homogeneous fatigue tests performed on a short glass fibre reinforced polyamide. The identified set of parameters appears to be not depending on the adopted initial values. The model as the parameters determined by the minimisation algorithm, are validated on a fatigue test performed with a different loading condition.

**Keywords:** Short glass fiber, fatigue damage, parameters identification.

## 1 Introduction

The present work is a contribution to the phenomenological modeling of fatigue damage in short glass fiber reinforced thermoplastic matrix composites. In such materials, the fatigue damage kinetic occurs according to three stages: i) material softening and damage initiation ii) coalescence and propagation of micro-cracks iii) macroscopic cracks propagation and material failure, [Sedrakian et al. 2002, Van Paepegem and Degrick 2002]. Different laws have been proposed to predict the damage accumulation in unidirectional or laminated polymer matrix composites [Van Paepegem and Degrick 2002, Ye 1989]. These models do not take into account the first stage of the damage kinetic observed in short glass fiber reinforced thermoplastics. From experimental investigation it is shown that during

the first few hundred cycles, the damage kinetic is mainly due to the material softening depending on the applied strain level. Based on the Ladevèze and Le Dantec approach [Ladevèze and Le Dantec 1992], the proposed modeling is an attempt to extend previous works by accounting for the important stiffness reduction observed during the early stage of the damage evolution. An inverse analysis is introduced in order to determine the set of parameters introduced in the current work. It is used experimental data obtained from tension-tension fatigue tests performed on a for short glass fiber reinforced thermoplastics and a cost function written in a least squares sense. It appears that the set of parameters computed from the analysis is not depending on the initial values. The modeling with the identified parameters is accurately compared to experimental data that have not been considered for the identification.

## 2 New Fatigue Damage Model

To take into account the observed three damage stages, a new polycyclic fatigue damage model is formulated on the basis of the meso model proposed by Ladevèze and Le Dantec [Ladevèze and Le Dantec 1992]. According to the continuum damage mechanics, the damage is introduced as an internal state variable coupled to elastic behaviour. Assuming a thin structure where ($\sigma_{33}=0$), made of an orthotropic material, elastic moduli of the damaged material are given by:

$$\begin{aligned} E_{11} &= E_{11}^0\left(1-d_{11}\right) \\ E_{22} &= E_{22}^0\left(1-d_{22}\right) \\ G_{12} &= G_{12}^0\left(1-d_{12}\right) \\ G_{13} &= G_{13}^0\left(1-d_{13}\right) \\ G_{23} &= G_{23}^0\left(1-d_{23}\right) \end{aligned} \tag{1}$$

Where $E_{11}$ (resp. $E_{22}$) is the Young's modulus in the longitudinal (resp. transverse) direction. $G_{12}$, $G_{13}$ and $G_{23}$ are the shear moduli. $d_{ij}$ are the damage variables associated to the corresponding moduli. The superscript 0 indicates initial values measured when $d_{ij}=0$. In the case where damage is disregarded, the elastic strain energy ($W_e$) is given by:

$$\begin{aligned} W_e = \frac{1}{2}\frac{1}{1-\nu_{12}\nu_{21}}\Big[\Big[E_{11}^0\varepsilon_{11}+\nu_{21}E_{11}^0\varepsilon_{22}\Big]\varepsilon_{11}+\Big[\nu_{12}E_{22}^0\varepsilon_{11}+E_{22}^0\varepsilon_{22}\Big]\varepsilon_{22}\Big] \\ +G_{12}^0\gamma_{12}^2+G_{13}^0\gamma_{13}^2+G_{23}^0\gamma_{23}^2 \end{aligned} \tag{2}$$

For a damaged material, the elastic strain energy becomes dependent on the state variables $d_{ij}$. Then, the strain energy ($W_d$) of a damaged material can be computed from Eq.( 2) by replacing ($E_{ij}^0$, $G_{ij}^0$) by the corresponding moduli ($E_{ij}$, $G_{ij}$) expressed in Eq. (1). One obtains:

$$
\begin{aligned}
W_d = & \frac{1}{2}\frac{1}{1-\nu_{12}\nu_{21}}\left[E_{11}^0(1-d_{11})\varepsilon_{11}\left\langle\varepsilon_{11}+\nu_{21}\varepsilon_{22}\right\rangle_+ + E_{11}^0\varepsilon_{11}\left\langle\varepsilon_{11}+\nu_{21}\varepsilon_{22}\right\rangle_-\right] \\
& + \frac{1}{2}\frac{1}{1-\nu_{12}\nu_{21}}\left[E_{22}^0(1-d_{22})\varepsilon_{22}\left\langle\varepsilon_{22}+\nu_{12}\varepsilon_{11}\right\rangle_+ + E_{22}^0\varepsilon_{22}\left\langle\varepsilon_{22}+\nu_{12}\varepsilon_{11}\right\rangle_-\right] \\
& + G_{12}^0(1-d_{12})\gamma_{12}^2 + G_{13}^0(1-d_{13})\gamma_{13}^2 + G_{23}^0(1-d_{23})\gamma_{23}^2
\end{aligned} \tag{3}
$$

Where (<A>+) and (<A>-) stand for the positive and negative parts of A, respectively. Thus, the damage affects $E_{11}$ (resp. $E_{22}$) only when $\varepsilon_{11}+\nu_{21}\varepsilon_{22}$ (resp. $\varepsilon_{11}+\nu_{21}\varepsilon_{22}$) is positive. This can be explained by the following. When the material is submitted to a compressive loading, transverse matrix cracks are supposed to be closed up and do not have any effect on the damage evolution. On the opposite, during tension loading those cracks are active and contribute to the development of the damage.

The thermodynamic dual variables $Y_{ij}$ associated to the damage variables $d_{ij}$ are deduced from the elastic strain energy $W_d$ of the degraded material:

$$
\begin{aligned}
Y_{11} &= -\frac{\partial W_d}{\partial d_{11}} = \frac{1}{2}\frac{1}{1-\nu_{12}\nu_{21}}E_{11}^0\varepsilon_{11}\left\langle\varepsilon_{11}+\nu_{21}\varepsilon_{22}\right\rangle_+ & Y_{12} &= -\frac{\partial W_d}{\partial d_{12}} = \frac{1}{2}G_{12}^0\gamma_{12}^2 \\
Y_{22} &= -\frac{\partial W_d}{\partial d_{22}} = \frac{1}{2}\frac{1}{1-\nu_{12}\nu_{21}}E_{22}^0\varepsilon_{22}\left\langle\varepsilon_{22}+\nu_{12}\varepsilon_{11}\right\rangle_+ & Y_{13} &= -\frac{\partial W_d}{\partial d_{13}} = \frac{1}{2}G_{13}^0\gamma_{13}^2 \\
& & Y_{23} &= -\frac{\partial W_d}{\partial d_{23}} = \frac{1}{2}G_{23}^0\gamma_{23}^2
\end{aligned} \tag{4}
$$

In the proposed modelling, the damage rate is assumed to be the sum of two components:

$$
\frac{d(d_{11})}{d(N)} = \frac{\alpha_{11}\beta_{11}}{1+\beta_{11}}\left(Y_{11}\right)^{\beta_{11}-1} + \lambda_{11}\left(Y_{11}\right)\left(e^{-(\delta_{11}N)}\right) \tag{5}
$$

$$
\frac{d(d_{22})}{d(N)} = \frac{\alpha_{22}\beta_{22}}{1+\beta_{22}}\left(Y_{22}\right)^{\beta_{22}-1} + \lambda_{22}\left(Y_{22}\right)\left(e^{-(\delta_{22}N)}\right) \tag{6}
$$

$$
\frac{d(d_{12})}{d(N)} = \frac{\alpha_{12}\beta_{12}}{1+\beta_{12}}\left(Y_{12}\right)^{\beta_{12}-1} + \lambda_{12}\left(Y_{12}\right)\left(e^{-(\delta_{12}N)}\right) \tag{7}
$$

$$
\frac{d(d_{13})}{d(N)} = \frac{\alpha_{13}\beta_{13}}{1+\beta_{13}}\left(Y_{13}\right)^{\beta_{13}-1} + \lambda_{13}\left(Y_{13}\right)\left(e^{-(\delta_{13}N)}\right) \tag{8}
$$

$$
\frac{d(d_{23})}{d(N)} = \frac{\alpha_{23}\beta_{23}}{1+\beta_{23}}\left(Y_{23}\right)^{\beta_{23}-1} + \lambda_{23}\left(Y_{23}\right)\left(e^{-(\delta_{23}N)}\right) \tag{9}
$$

The first contribution, scaled by $(Y_{ij})^{\beta ij\text{-}1}$ in Eqs. (1.5) to (1.9), is derived from the Norton dissipation potential. Note that in a previous work from Sedrakian et al [Sedrakian et al. 2002] the damage evolution is only described by this first term. The second component is introduced in order to describe the rapid stiffness

reduction occurring during cyclic loading of reinforced thermoplastics [Nouri et al 2009]. The developed model is then a complete model in the sense that the entire damage process (3 stages) could be described. The instantaneous state variables $d_{ij}(N)$ are obtained by numerical integration of Eqs. (1.5) to (1.9), with the initial conditions $d_{ij}(N=0)=d^{qs}{}_{ij}$. These initial values are function of the imposed displacement. In the case where the applied strain ($\varepsilon^{app}{}_{ij}$) is below a threshold value associated to the beginning of the damage process in the $(i,j)$ direction, ($d^{qs}{}_{ij}=0$). From equations (1.5) to (1.9), it appears that the proposed model involves 20 parameters in the general case of a 3–D structure. Nevertheless, it should be mentioned that the model is essentially developed for thin composite structures. In that particular case, relationships governing the damage evolution are reduced to Eqs. (1.5) to (1.7) and only 12 parameters have to be identified namely, 4 parameters per damage variable. In the next section, an identification procedure is adopted to reach this goal.

# 3 Experimental Identification

Material damage parameters identification cannot be achieved without experimental tests involving the three stages of damage. In the present paper, we focus on longitudinal tension-tension tests leading to only a longitudinal damage $d_{11}$. For simplicity in the notation, $d_{11}$ is denoted hereafter $d$ and corresponds to the longitudinal damage in Eq. (1.5). In the same way, $\alpha$, $\beta$, $\lambda$ and $\delta$ substitute $\alpha_{11}$, $\beta_{11}$, $\lambda_{11}$ and $\delta_{11}$ in Eq. (1.5).

## *3.1 Experimental Procedure*

We consider fatigue tests performed in tension-tension. The studied composite material is a polyamide thermoplastic reinforced short glass fibre, denoted by TP-GF hereafter. The reinforcement makes the material highly resistant to abrasion, compression, tension or bending. The specimens used in the static and fatigue tensile tests were cut from thin plates. The geometry and dimensions of the tension specimens are shown in Figure 1. Fatigue tests were strain controlled and carried out using a servo-hydraulic machine. The imposed displacement wave was sinusoidal with constant amplitude. All tests were performed at room temperature. The mechanical properties of the material have been extracted from static tension tests. Some of the properties are given in Table 1.

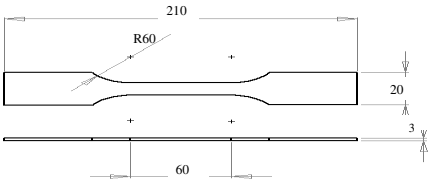


**Fig. 1** Specimen used for tension tests (dimensions in mm)

**Table 1** Monotonic mechanical properties of the studied material and standard deviations

| Material | $E^0$ (MPa) | $\varepsilon_{damage\ Threshold}$(%) | $\varepsilon_{Rup}$(%) | $\sigma_{UTS}$(MPa) |
|---|---|---|---|---|
| TP-GF longitudinal direction | 7042. (370) | 0.7 (0.02) | 5. (0.4) | 114. (6) |

Experimental cyclic tests are driven by an applied displacement, see Figure 2. It is introduced the maximum strain $\varepsilon_{max}$ and the minimum strain $\varepsilon_{min}$. It is usually defined the fatigue ratio by $R=\varepsilon_{min}/\varepsilon_{max}$. Note that $\varepsilon_{rup}$ denotes the maximum strain reached when the material fails. Three strain levels ($\varepsilon_{max}=20\%\varepsilon_{rup}$, $\varepsilon_{max}=30\%\varepsilon_{rup}$ and $\varepsilon_{max}=40\%\varepsilon_{rup}$) have been conducted using three specimens for each different levels. The ratio R remains the same for the different configuration (R=0.3). The frequency is 2Hz. Some properties are summarized in Table 2.

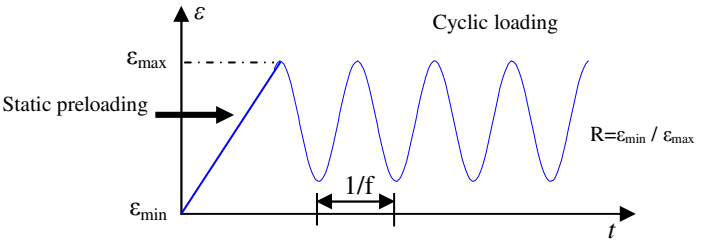


**Fig. 2** Strain history obtained from an imposed displacement test. Note that the static pre-loading (up to the point F) could give rise to an initial damage representing the quasi-static damage (denoted by $d_{qs}$ in the current work).

**Table 2** Monotonic mechanical properties of fatigue test

| | Test 20% | Test 30% | Test 40% |
|---|---|---|---|
| $\varepsilon_{rup}$ | 5 | 5 | 5 |
| $E^0$ | 7600 | 7200 | 6900 |
| $d_{qs}$ | 0.05 | 0.08 | 0.10 |

It is shown on Figure 3 the evolution of $d$ versus $N$ obtained from experimental fatigue tension-tension tests at different $\varepsilon_{max}$ ($\varepsilon_{max}=20\%$,$\varepsilon_{max}=30\%$, $\varepsilon_{max}=40\%$). It is observed that even if data are quite scattered, an increase in $\varepsilon_{max}$ leads to an increase in the damage rate, and an enhanced $d_{qs}$. This is due to a more cumulative damage occurring when the maximum strain passes from $20\%\varepsilon_{rup}$ to $30\%\varepsilon_{rup}$ to $40\%\varepsilon_{rup}$. In Figure 2, the point F defines the end of the quasi-static step. It is the highest for $\varepsilon_{max}=40\%\varepsilon_{rup}$ and the lowest for $\varepsilon_{max}=20\%\varepsilon_{rup}$. In the latter case, less damage is cumulated up to the point F, and $d_{qs}$ is then reduced. From Eq.(1.4) with $Y_{11}=Y$, in the case of an uniaxial strain test ($\varepsilon_{22}=0$), the thermodynamic variable $Y$ is increased when $\varepsilon_{11}$ increases. That leads to an increase in $d(d)/d(N)$, see Eq.(1.5) with $d_{11}=d$.

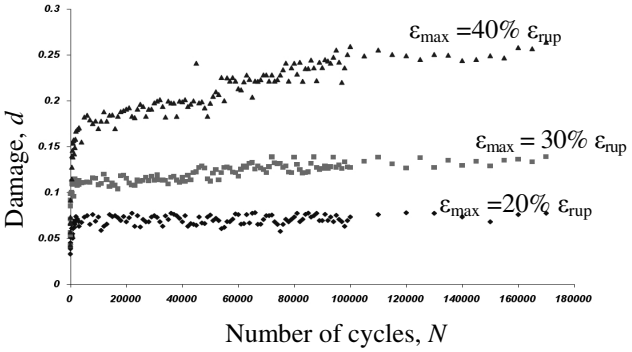


**Fig. 3** Experimental results of the evolution of the damage $d$ versus the number of cycles $N$. The studied composite material was subjected to tension-tension displacement controlled fatigue test. Three maximum applied strains $\varepsilon_{max}$ were considered: 20%, 30% and 40% of the total fracture strain measured during a static tensile test. The fatigue ratio was R=0.3.

## *3.2 Identification of Parameters*

The goal is to extract the material parameters from experimental data. An objective function representing, in the least squares sense, the difference between experimental and numerical data [Gavrus et al.1996] has been built and minimised. The cost function is written as:

$$S(\underline{P}) = \frac{\sum_{i=1}^{a}\left[d_i^{comp}(\underline{P}) - d_i^{exp}\right]^2}{\sum_{i=1}^{a}\left(d_i^{exp}\right)^2} \tag{10}$$

Where $a$ is the number of experimental data. $d_i^{exp}$ measures the damage in the longitudinal direction and $d_i^{comp}$ is the computed value obtained from the modelling (Eq 1.5) with $d_{11}=d$. $\underline{P}$ is the parameter vector that contains (α, β, λ, δ).

The minimisation of the cost function is an iterative procedure. At each step, the vector $\underline{P}$ is re-estimated ($\underline{P}$ becomes $\underline{P}+\Delta\underline{P}$) and the cost function $S$ is re-evaluated. $\underline{\Delta P}$ is computed by using a Gauss-Newton algorithm. The iterative procedure is stopped when two consecutive values of the cost function satisfy: $\left\|S(\underline{P}+\Delta\underline{P}) - S(\underline{P})\right\| < 10^{-5}$. Namely, the cost function becomes stationary. The parameters α, β, λ and δ are identified by using experimental data obtained from tests corresponding to $\varepsilon_{max}=30\%\varepsilon_{rup}$ and $\varepsilon_{max}=40\%\varepsilon_{rup}$. The comparison between experimental data used for the identification strategy and the computed damages are presented on Figure 4. Moreover, it has been assessed that the identification procedure does not depend on the initial values of α, β, λ and δ.

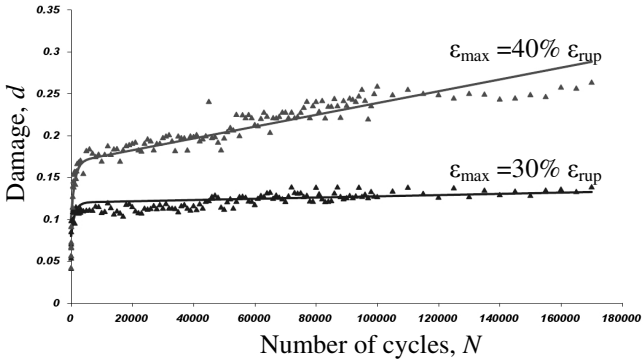


**Fig. 4** Comparison between experimental and calculated damage data for two configurations ($\varepsilon_{max}$=30%$\varepsilon_{rup}$ and $\varepsilon_{max}$=40%$\varepsilon_{rup}$)

Finally, the set of parameters determined by the inverse procedure is validated on the experimental curve for the case where $\varepsilon_{max}$=20%$\varepsilon_{rup}$. Figure 5 shows the comparison between experimental data and numerical calculations for the parameters computed from the identification procedure.

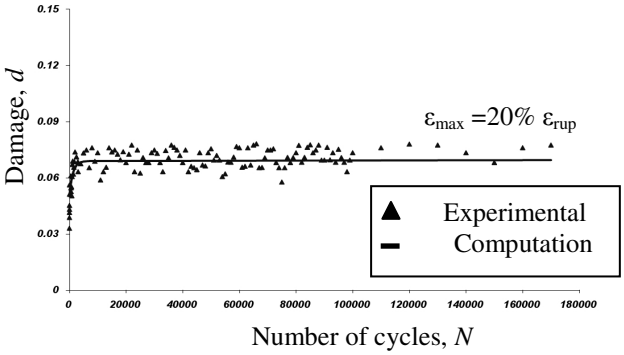


**Fig. 5** Comparison between experimental and calculated damage data for $\varepsilon_{max}$=20% of $\varepsilon_{rup}$. This validates the identified set of parameters

## 4 Conclusion

In this work, a new cumulative fatigue damage model in short glass fibre reinforced thermoplastics is developed. These composites are characterised by an evolution of the damage in three stages. The new model is able to capture the first stage of damage specific to the composite materials with thermoplastic matrix.

This paper presents a first identification strategy: homogeneous tensile fatigue tests have been performed in the longitudinal direction. Three strain controlled fatigue tests at different levels have been carried-out to identify the four parameters

governing the evolution of the longitudinal damage. The parameters are identified by using experimental data from 2 different tests at different strain levels. The model, insensitive to the initial values, is validated on a third fatigue test.

A second identification strategy is currently ongoing. It is based on the use of optical whole-field displacement/strain measurements by digital image correlation coupled to an inverse method from one single coupon. It is worth noting that the mechanical test must give rise to heterogeneous stress/strain fields. Indeed, in this case, the constitutive parameters are expected to be all involved in the response of the specimen.

## References


Sedrakian, A., Ben Zineb, T., Billoet, J.L.: Contribution of industrial composite parts to fatigue behaviour simulation. International Journal of Fatigue, 307–318 (2002)

Gagel, A., Fiedler, B., Schulte, K.: On modelling the mechanical degradation of fatigue loaded glass-fibre non-crimp fabric reinforced epoxy laminates. Composites Science and Technology 66, 657–664 (2006)

Van Paepegem, W., Degrieck, J.: A new coupled approach of residual stiffness and strength for fatigue of fibre-reinforced composites. International Journal of Fatigue 24, 747–762 (2002)

Degrieck, J., Van Paepegem, W.: Fatigue damage modeling of fibre-reinforced composite materials: Review. Applied Mechanics Review 54, 279–299 (2001)

Ye, L.: On fatigue damage accumulation and material degradation in composite materials. Composites Sciences and Technology 36, 339–350 (1989)

Ladevèze, P., Le Dantec, E.: Damage modelling of the elementary ply for laminated composites. Composites Science and Technology 43, 257–267 (1992)

Nouri, H., Meraghni, F., Lory, P.: A new thermodynamical fatigue damage model for short glass fibre reinforced thermoplastic composites. In: 16th International Conference on Composite Materials, Kyoto (July 2007)

Cooreman, S., Lecompte, D., Sol, H., Vantomme, J., Debruyne, D.: Elasto-plastic material parameter identification by inverse methods: Calculation of the sensitivity matrix. International Journal of Solids and Stuctures (November 2006)

Claire, D., Hild, F., Roux, S.: A finite element formulation to identify damage fields: the equilibrium gap method. International Journal for Numerical Methods in Engineering 61, 189–208 (2004)

Gavrus, A., Massoni, E., Chenot, J.L.: An inverse analysing a finite element model for identification of rheological parameters. Journal of Materials Processing Technology 60, 447–454 (1996)